Advances in Concrete Construction, *Vol. 8, No. 2 (2019) 77-90*
DOI: https://doi.org/10.12989/acc.2019.8.2.077

Experimental damage evaluation of prototype infill wall based on forced vibration test

Onur Onat*

Department of Civil Engineering, Munzur University, Aktuluk Campus, Tunceli, Turkey

(*Received July 23, 2018, Revised February 21, 2019, Accepted March 30, 2019*)

Abstract. This paper aims to investigate vibration frequency decrease (vibration period elongation) of reinforced concrete (RC) structure with unreinforced infill wall and reinforced infill wall exposed to progressively increased artificial earthquake load on shaking table. For this purpose, two shaking table experiments were selected as a case study. Shaking table experiments were carried on 1:1 scaled prototype one bay one storey RC structure with infill walls. The purpose of this shaking table experiment sequence is to assess local behavior and progressive collapse mechanism. Frequency decrease and eigen-vector evolution are directly related to in-plane and out-of-plane bearing capacities of infill wall enclosure with reinforced concrete frame. Firstly, frequency decrease-damage relationship was evaluated on the base of experiment results. Then, frequency decrease and stiffness degradation were evaluated with applied Peak Ground Acceleration (PGA) by considering strength deterioration. Lastly, eigenvector evolution-local damage and eigenvector evolution-frequency decrease relationship was investigated. Five modes were considered while evaluating damage and frequency decrease of the tested specimens. The relationship between frequency decrease, stiffness degradation and damage level were presented while comparing with Unreinforced Brick Infill (URB) and Reinforced Infill wall with Bed Joint Reinforcement (BJR) on the base of natural vibration frequency.

Keywords: frequency decrease; forced vibration frequency; infill wall; shaking table experiment; eigenvector evolution

1. Introduction

Dynamic characteristics of a structure strongly affect seismic action of the structure. One of the most important dynamic characteristics is the natural vibration frequency. On this basis, many numerical studies have been performed to develop empirical formulation and experimental studies have been performed to obtain a natural vibration frequency of RC buildings, especially in relation to the height of an investigated structure (Masi and Vona 2010). Natural vibration frequency mainly depends on mass, stiffness, strength and associated factors which affect listed parameters such as dimensions in height and plan or vertical irregularities, cross section properties of main bearing elements, number of storeys, infill panel properties and stiffness (Eleftheriadou *et al*. 2012, Onat 2019). For listed reasons, the fundamental frequency or period of buildings is important to assess for the newly designed buildings, existing ones and progressively damaged ones (Chiauzzi *et al*. 2012). In a performance assessment with numerous numbers of mesh, numerical analysis by using a software to determine the natural vibration frequency of each selected structure is unfeasible and ineffective. Thus, available experimental results or simplified empirical equations and semi-empirical methods are effective (if available for all condition), and more applicable to different types of buildings with wide variety of property (Crowley and Pinho 2004). For this purpose, Goel and Chopra (1997, 1998, 2000) evaluated available RC structures with and without shear dominant wall system and proposed an equation to estimate ambient vibration period. However, traditional FE modeling of RC buildings, which are commonly used in strength analysis and design, give the structures more flexible than they are. The reason for this is the fact that the effect of non-bearing elements like the infills. In reality, non-structural elements contribute to the stiffness of the overall structural system. These secondary elements lead to obtain shorter time periods as they are measured during any ground excitation (Amanat and Hoque 2006). On this basis, the elastic and yield natural vibration period values of existing RC buildings in different height in European countries were calculated by using eigenvalue analysis. The mentioned study led to a simplified period-height relationship for using in the assessment of existing RC structures considering the presence of infills by Crowley and Pinho (2004). Equations and relationship with height and period of the structure are provided by Gallipoli *et al*. (2009), Guler *et al*. (2008), Al-Nimry *et al*. (2014), Vidal *et al*. (2014) and Salameh *et al*. (2016) to simulate the current design and construction practice of each studied country in Italy, Turkey, Jordan, Spain and Lebanon, respectively for available structure under current condition not for damaged state. For instance, Gallipoli *et al*. (2009) defined an empirical equation for undamaged buildings in Italy. Moreover, building stock in Turkey was evaluated to derive an equation by using ambient vibration tests for a fully elastic condition (Guler *et al*. 2008). Moreover, Kocak and

*Corresponding author, Associate Professor
E-mail: onuronat@munzur.edu.tr, onuronatce@gmail.com

ISSN: 2287-5301 (Print), 2287-531X (Online)

Yıldırım (2011), Kocak *et al*. (2018) proposed an equation to estimate natural vibration period considering infill wall and infill wall gaps for fully elastic limit. However, these suggested equations by Kocak and Yıldırım still available for undamaged condition of a structure. Effect of location of soft storey on vibration period and soil type were investigated in elastic range with numeric model by Asteris *et al*. (2015).

Structural systems start oscillation for a long period after cracking of structural elements. Cracking of structural and/or non-structural members can occur during the service life of the structure under gravity load or the effect of any external event. For this reason, calculating vibration period of the structure with damaged or cracked stiffness is even more necessary (Masi and Vona 2010). For this purpose, associated investigations were performed by many researchers like Masi and Vona (2010). Experimental in situ and ex situ test results from structures which suffered from Basilicata 1998 and Molise 2002 earthquakes caused from moderate to heavy damages under seismic actions are demonstrated, and the relationship between damage level and period elongation are reported (Masi and Vona 2010). Ditommaso *et al*. (2013) proposed an equation which includes structural and non-structural member damage depends on height-period relationship. In the mentioned study, 5 damage levels were defined and, period elongation and stiffness degradation were presented on this basis (Ditommaso *et al*. 2013). Vidal *et al*. (2014) measured a series of natural vibration period of structural system before and after 2011 Lorca earthquake sequence to derive an empirical equation for fast evaluation of structural damage and dynamic properties of available structural stock.

The goal of this paper is to present frequency of an infilled prototype RC framed structure in elastic state and damaged state state. Moreover, Stiffness degradation of an infilled prototype RC framed structure was investigateddue to local out-of-plane failure resulted from in-plane damage with applied PGA by considering strength deterioration. For this purpose, a series of shaking table experiments were carried out on two prototype RC one bay one storey 1:1 scaled structure with infill walls. One of the RC infill walls is Unreinforced Brick (URB) infill wall, the other is reinforced infill wall with Bed Joint Reinforcement (BJR). Frequency decrease, in other words period elongation, under forced vibration level after each shaking table experiment phase was discussed in this paper.

2. Experimental campaign and testing protocol

The purpose of these shaking table experiment series is to assess the out-of-plane response and local failure mechanism of brick infill walls and to take suitable preventing measures according to their progressive collapse mechanisms. The experimental tests were performed on the shaking table of the Portuguese National Laboratory for Civil Engineering (LNEC), in Lisbon (URL-1). The large capacity shaking table has a three degree of freedom (TDOF), where the three translations are digitally controlled, and the three rotations are passively restrained, having dimensions in plan of 5.6 m×4.6 m and allowing for payloads up to 40 metric tons. Allowable maximum displacement is 175 mm through all three dimensions. A distinctive feature of this experimental facility is having three reaction walls surrounding the shaking table, as shown in Fig. 1, which allows for a number of combinations of test setups.

Fig. 1 Schematic view of 3 degree of freedom shaking table and reaction walls at LNEC (Onat *et al*. 2018)

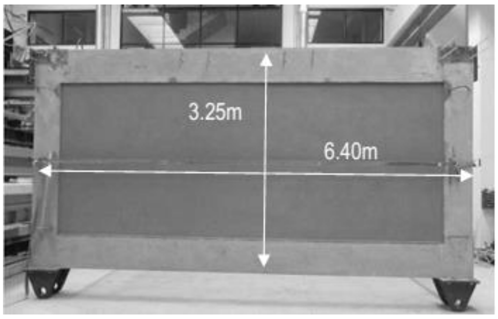

(a) Dimensions of the test specimens


(b) Brickwork

Fig. 2 Physical view, dimensions and brickwork of specimens

The test setup on the shaking table uses the reaction walls and the shaking table simultaneously reaction walls and the shaking table. This test set up is called “Testing device for Innovative Masonry infills (TIM)”, as described in Leite *et al*. (2015).

The brick infill specimens are depicted in Fig. 2. Brick infills are surrounded by an RC frame with external dimensions of 6.40 m×3.25 m. The beam elements of the frame had cross-section dimensions of 0.5×0.3 m^2 and the column elements had 0.4×0.3 m^2 cross-section dimensions of 0.4×0.3 m^2. Infill wall specimens were tested simultaneously for in-plane (Longitudinal direction) and out-of-plane (Transversal direction) directions under

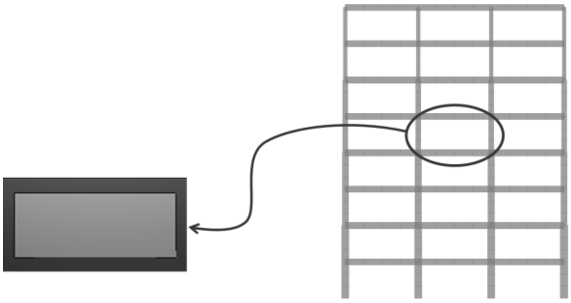

Fig. 3 Isolated prototype for shaking table experiments

Fig. 4 Test setup, specimen and TIM (Onat *et al.* 2018)

dynamic actions, representing the response of a 5th floor frame panel of an 8-story RC building as presented in Fig. 3. Therefore, the columns have a centered, and adherent, pre-stress of 360 kN, representing the vertical load from the floors above. The brick units have dimensions of 30×20×22 cm^3. Both walls were plastered, and the bed joint reinforcement was connected with the frame using conventional ribbed steel bars.

Depicted specimens, as shown in Fig. 2, were tested simultaneously for in-plane and out-of-plane dynamic actions, representing the response of a fifth-floor frame panel of a generic eight-story RC building as seen in Fig. 3.

The innovative test setup mainly consists of a rigid steel solid frame, with hollow rectangular cross-section, which moves rigidly together with the shaking table. The steel frame is mounted to the specimen's upper beam to allow rigid body motion in the transverse (out-of-plane) direction, while a system of rollers allows for an independent motion in the longitudinal (in-plane) direction.

The in-plane motion allows the lower beam an inter-story drift time-history on the frame by restraining the upper beam's longitudinal motion through a strut connecting it to the reaction wall as depicted in Fig. 4, and by imposing the displacement of the shaking table on the lower beam of the frame. The connection between the strut and the reaction wall is constructed via a three-dimensional pyramidal support, as presented in Fig. 4, which transfers the strut's reaction on the reaction wall. A long rod then links the pyramidal support to the RC frame's upper beam with hinge connection. Moreover, the upper beam also has 360 kN of centered pre-stress for withstanding pull-push force actions.

Besides, the out-of-plane motion consists of a rigid-body vibration of the entire RC frame, reproducing the story

Table 1 Seismic input intensities at each stage for the URB model

Stage	Return Period (Years)	PGA (g)	
		Transverse	Longitudinal
1	75	0.04	0.08
2	225	0.18	0.29
3	475	0.39	0.40
4	975	0.53	0.64

(a) Bed joint reinforcement

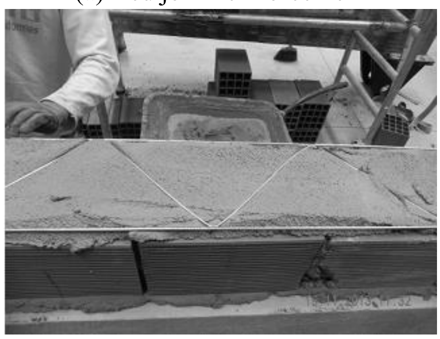

(b) During construction

Fig. 5 Bed joint reinforcement and construction of the model (Onat *et al.* 2018)

absolute accelerations and therefore inducing high-frequency inertia forces perpendicular to the brick infill panel and leading to a local vibration of the infill wall. Note that this shaking table motion is transmitted to the upper beam through the rigid steel frame of TIM.

The seismic input motions for the specimens corresponds to the response of a representative building model. The considered response history in terms of interstory drift at the 5th floor for the seismic input corresponds to the shaking table motion to be applied in the longitudinal direction.

A total of 24 accelerometers were placed in the longitudinal and transverse directions. The seismic input was applied to the specimens by test stages of increasing intensity. Table 1 summarizes, for the URB model, the applied seismic input intensities of each stage in terms of peak horizontal accelerations for both in-plane and out-of-plane directions.

It should be noted that the input motion in the longitudinal and transverse directions do not maintain the same proportion at all stages because of the inevitable gaps and slip motions existing in the connection of the model to the reaction wall. Moreover, the rotations of the shaking

Table 2 Seismic input intensities at each stage for the BJR model

Stage	Return Period (Years)	PGA (g)	
		Transverse	Longitudinal
1	75	0.05	0.08
2	225	0.15	0.36
3	475	0.38	0.54
4	2475	0.74	0.64

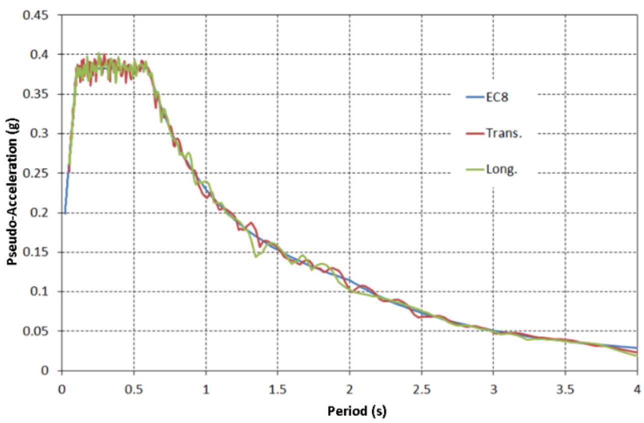

Fig. 6 Longitudinal, transversal and EC8 spectrum of reference quake

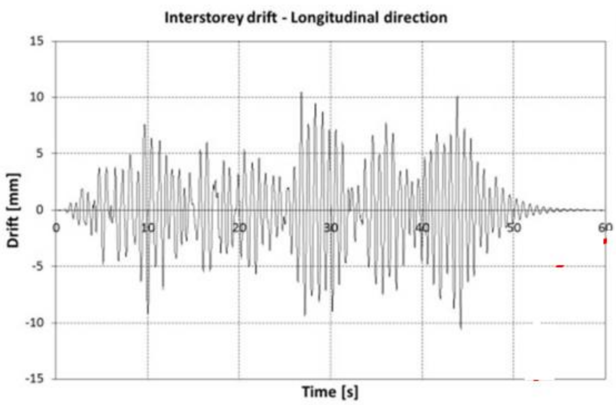

Fig. 7 Interstory drifts through the in-plane direction

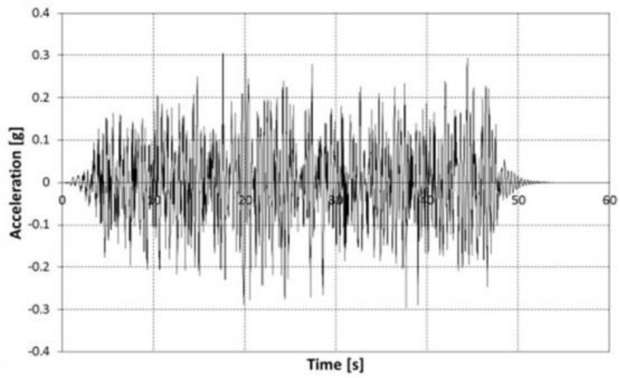

Fig. 8 Absolute acceleration in transversal direction

table are passively restrained but not completely prevented, which contributes to the need of imposing a longitudinal motion to the shaking table that is larger than the drift actually sustained by the frame.

Fig. 5 depicts the construction of the second specimen, using the bed joint reinforcement technique. The type of reinforcement used in bed joint is Bekaert Murfor RND/Z 5-200, with a characteristic tensile strength of 500 MPa. This second specimen was tested also in four stages, as described in Table 2, since by the end of stage 3 the drift expected for stage 5 was already attained. This difference is due to the changes in the stiffness of the strut connection to the reaction wall between the two models, with the stiffness of the auxiliary structure being larger in the BJR model.

Bi-directional seismic action was artificially generated and adjusted to the Spectrum of the EC8 for Lisbon. In addition, different levels of the seismic action were considered. Reference earthquake spectrum can be seen in Fig. 6 and return period of artificially produced earthquake can be seen in Table 3.

Besides, the absolute maximum acceleration measured in the out-of-plane direction corresponds to the shaking table transverse motion transmitted by TIM to the brick infill panel enclosed with the RC frame. Inter story drift through in-plane direction and acceleration through out-of-plane direction can be seen in Fig. 7 and Fig. 8, respectively.

3. Dynamic identification with forced vibration test

Forced vibration test was performed on the two models before shaking table experiments and after each achieved test level to extract mode frequencies and mode shapes. Transversal and longitudinal mode shapes were extracted. Transversal mode shapes were measured with twelve accelerometers on infill wall and eight accelerometers on RC frame. Longitudinal mode shapes were measured with two accelerometers. After the construction of the structure, PCB Piezoelectric accelerometers were placed on the infill wall and RC frame.

Location of accelerometers on the infill wall and enclosure can be seen in Fig. 9.

There are four vertical alignments and four horizontal alignments on the test specimens as seen in Fig. 9. The purpose of these alignments is to give a coordinate to each accelerometer and to plot the eigenvectors in order to observe the eigenvector evolution of the infill wall. There are totally twelve accelerometers mounted on the infill wall to capture out-of-plane behavior of the specimen. To plot out-of-plane behavior clearly, virtual axis was created both in horizontal direction and longitudinal direction. Axis was numbered and demonstrated with abbreviations. Horizontal axis was demonstrated with Horizontal Alignment (HA) and vertical axis was demonstrated with Vertical Alignment (VA) as presented in Fig. 9. There is also a supplementary equipment called Strut. The mission of Strut in these shaking table experiments is to keep the test specimens stable along the in-plane direction. The term in-plane direction refers to the longitudinal direction of the test specimens, and the term out-of-plane direction refers to the direction perpendicular to the planar surface of the infill wall.

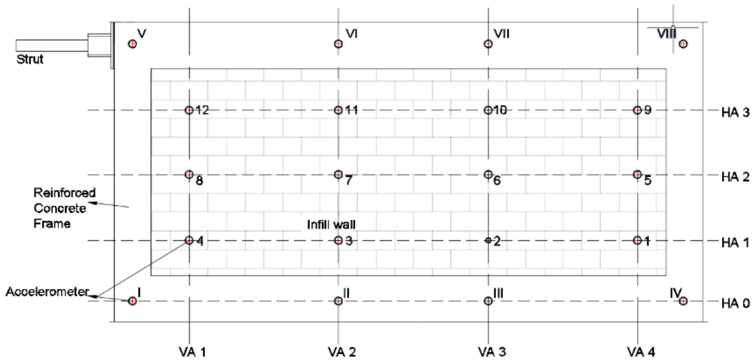

Fig. 9 Location of accelerometers (Onat and Gul 2018)

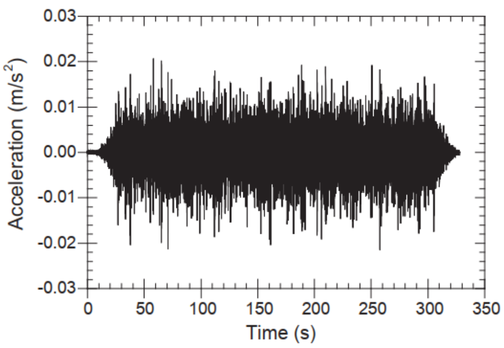

Fig. 10 Loading history of shaking table for dynamic identification

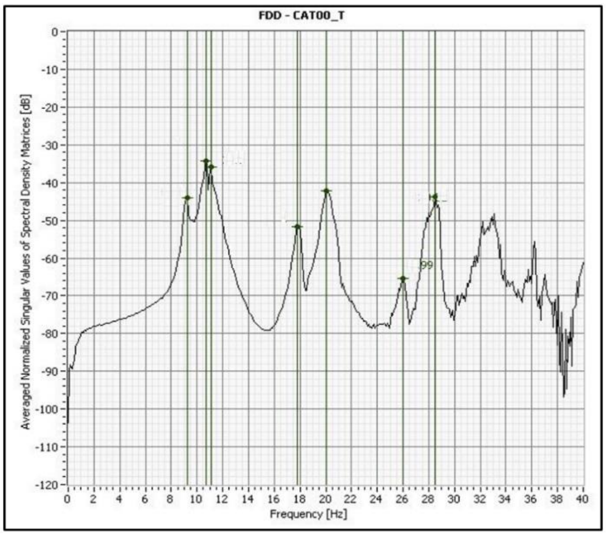

Fig. 11 Spectral density matrices of the dynamic identification set for transversal direction undamaged condition

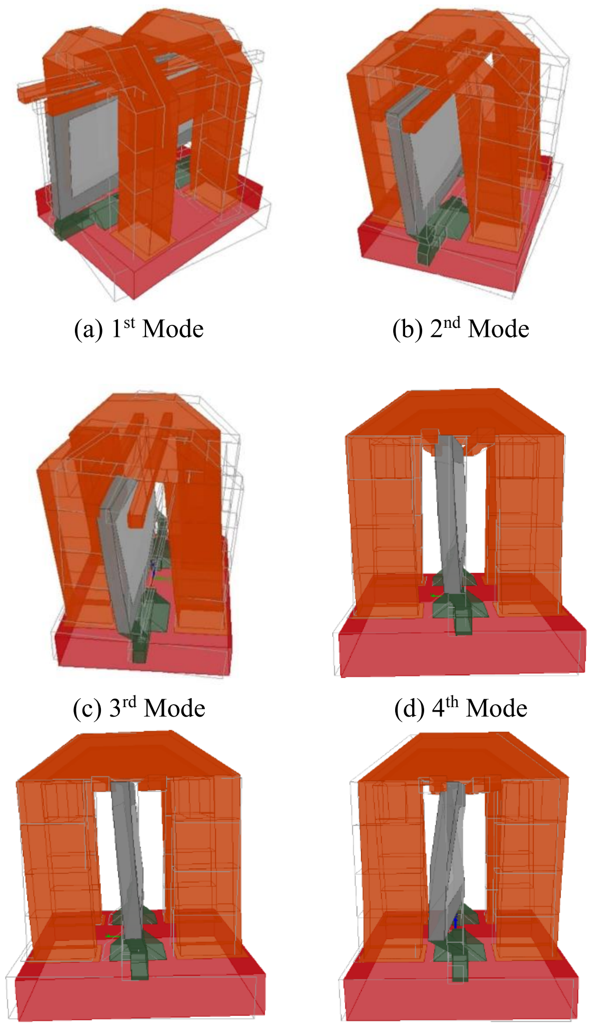

(a) 1st Mode (b) 2nd Mode

(c) 3rd Mode (d) 4th Mode

(e) 5th Mode (f) 6th Mode

Fig. 12 Transversal mode shapes of tested specimen and auxiliary support

Forced vibration tests were implemented, after each loading protocol during 330 second, considering 0-100 Hz frequency range as presented in Fig. 10. The signals acquired from the accelerometers were accumulated in data acquisition system and then transferred into the LNEC-SPA (Mendes and Oliveira 2008) software's for signal processing.

Averaged normalized singular values of spectral density matrices (ANSVSDM) and the average of auto spectral densities (AASD) of the data set that were obtained by Enchased Frequency Domain Decomposition (EFDD) method for undamaged condition are given in Fig. 11.

The EFDD technique is the extension of FDD technique. FDD method is based on using a single frequency line from the Fast Fourier Transform analysis (FFT). The accuracy of predicted forced vibration frequency depends on the FFT resolution and no modal damping is calculated. Comparing FDD with EFDD, EFDD

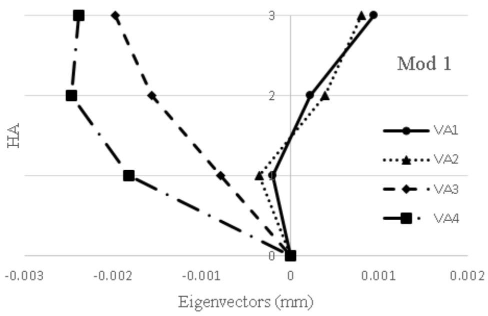

(a) Mode-1

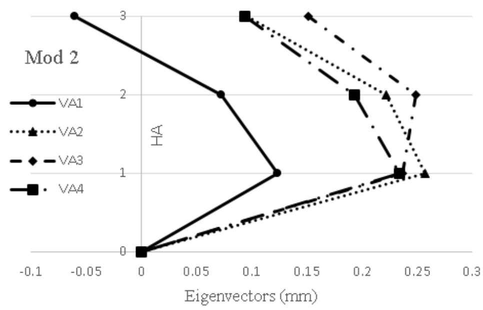

(b) Mode-2

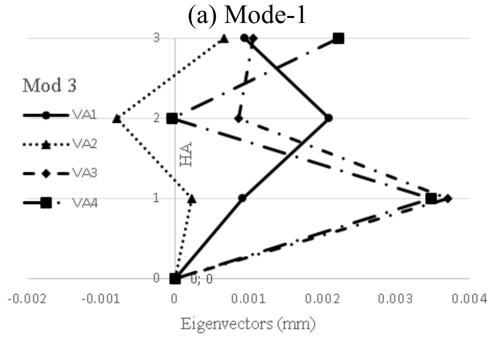

(c) Mode-3

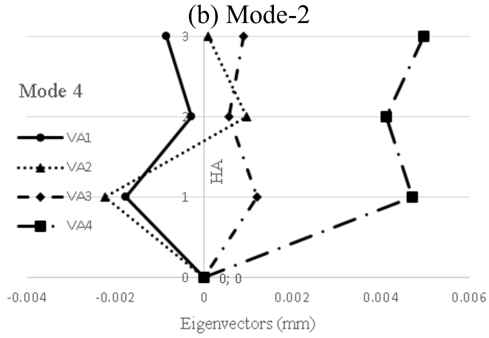

(d) Mode-4

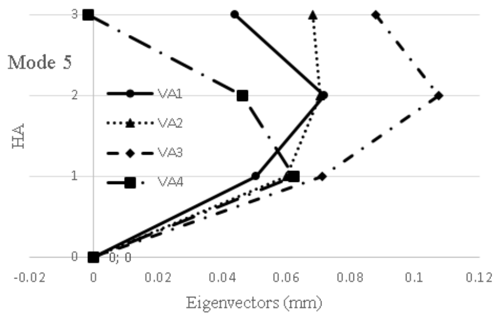

(e) Mode-5

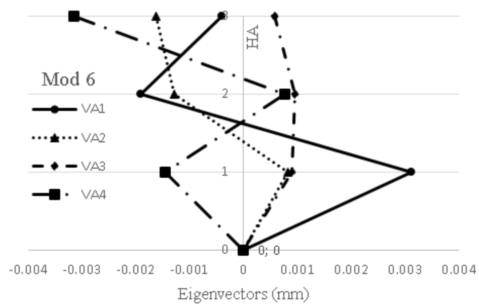

(f) Mode-6

Fig. 13 Transversal eigen-vectors of undamaged URB model

gives an improved prediction of frequencies and mode shapes (Altunışık *et al*. 2011, Sevim *et al*. 2011a, Zhang *et al*. 2011). EFDD method was developed on the base of the Complex Mode Identification Function (CMIF), which is a stochastic technique that is based on the evaluation of the spectral matrix *S*, determined by placing on the main diagonal the auto-spectral densities S_{ii} of each measurement point, while on the out-of-diagonal terms, the cross-spectral densities S_{ij} placed into relation all the measurements even if obtained from different dynamic tests. The singular values, a function of the changing frequency, are assumed as a modal indicator. Under some assumptions (white noise excitation, low damping and orthogonal mode shape for close modes) it can be shown that the singular value curves in the frequency domain belonging to the diagonal of ΣS are auto-spectral density functions of a Single Degree of Freedom (SDOF) system with the same frequency and damping as the structural vibration modes. Thus, the peaks of the singular value curve, in the frequency domain, allow the identification of the system frequencies and animation is performed immediately (Su *et al*. 2012, Sevim *et al*. 2011b Foti *et al*. 2014, Yu *et al*. 2014). For the listed reasons, EFDD was used to extract mode frequencies for TIM test set-up.

Extracted mode shapes for transversal direction can be seen in Fig. 12 for undamaged condition.

Effect of damage level on mode shape evolution was investigated on the base of the mode shapes depicted in Fig. 13 are benchmark for damage evolution.

Eigenvectors of undamaged BJR specimen can be seen in Fig. 14.

4. Results and discussion

4.1 Model-I: URB

Following the testing sequence as presented in section 2, Table 1 and Table 2, it was aimed to gather a series of data related to local out-of-plane failure mechanism of infill walls. Out-of-plane failure of failure of infill wall is directly related to in-plane damage level. For this reason, longitudinal (in-plane) frequency and transversal (Out-of-plane) frequency decrease was presented together as plotted in Table 3 and Table 4, respectively.

After shaking table experiments of URB model, artificial earthquake loads were applied to the specimen at four different level. Four dynamic identifications were

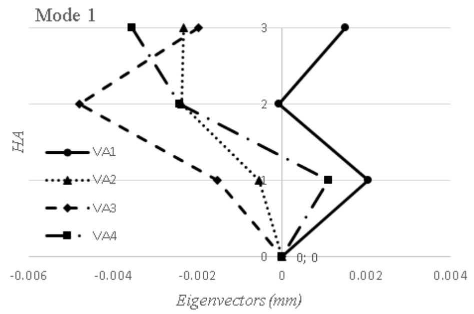

(a) Mode-1

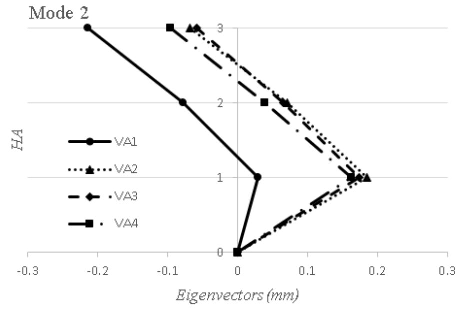

(b) Mode-2

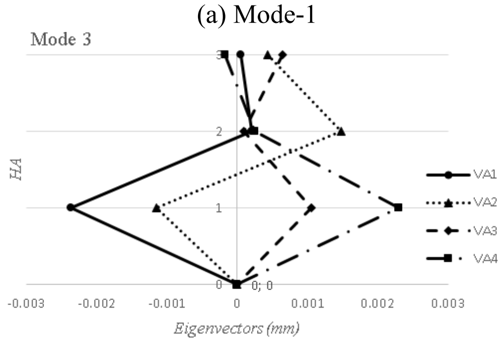

(c) Mode-3

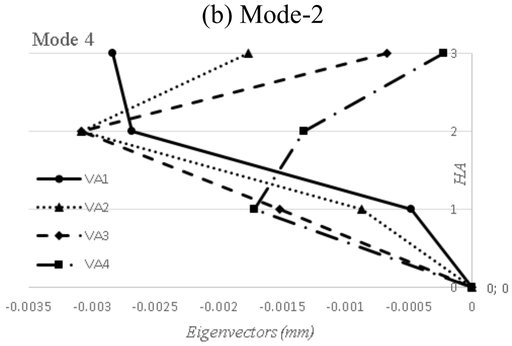

(d) Mode-4

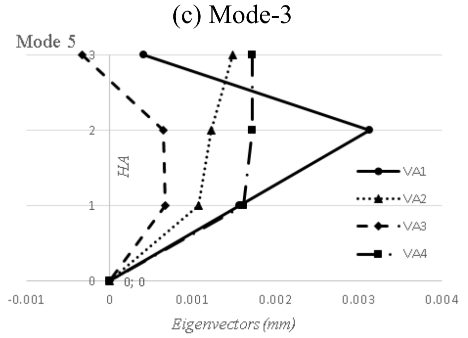

(e) Mode-5

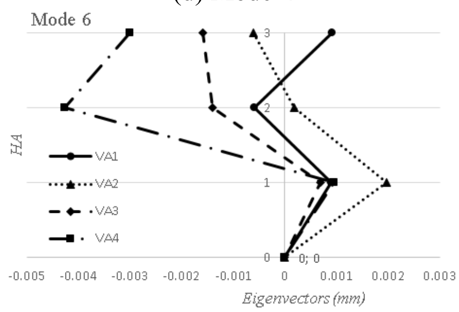

(f) Mode-6

Fig. 14 Transversal eigen-vectors of undamaged BJR model

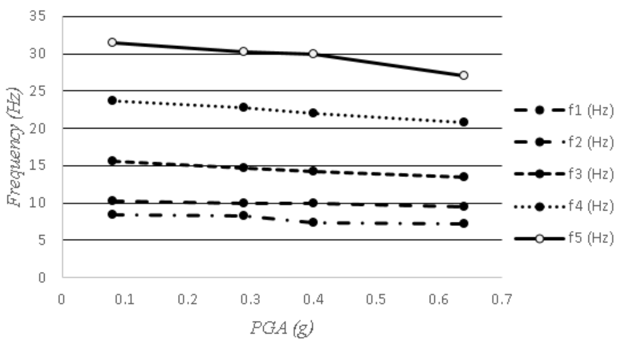

(a) In-Plane URB

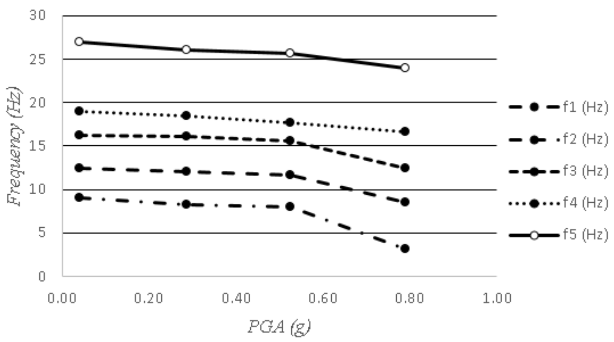

(b) Out-of-plane URB

Fig. 15 Frequency change of URB for five modes during in-plane and out-of-plane excitation

presented in both Table 3 and Table 4. These presented identifications have their own abbreviations to represent damage levels: DS_0 present dynamic identification belongs to initial damage status without damage. DS_1 (Slight Damage) presents first damage state after second phase earthquake load corresponds to 0.18 g and 0.29 g in transversal and longitudinal direction, respectively for URB model. In addition, 0.15 g in transversal and 0.36 g in longitudinal direction for BJR model. However, earthquake level with 75 years return period has not any damage effect on the specimens both for URB and BJR models.

Fig. 15 (a) and (b) show the reduction of the forced vibration frequency of the five modes of the URB model both in-plane and out-of-plane direction obtained through the dynamic identification tests, respectively. After seismic test with 225 years return periods, the steepest drop of frequency was measured at the first mode. The highest frequency drop was measured after the seismic test with

Table 3 Longitudinal frequency of URB

Damage State	f_1	f_2	f_3	f_4	f_5	Δf_1 (%)	Δf_2 (%)	Δf_3 (%)	Δf_4 (%)	Δf_5 (%)	Avg. Δf (%)
DS_0 (Undamaged, before test, Hz)	8.4	10.2	15.6	23.6	31.5	-	-	-	-	-	-
DS_1 (Slight damage, Hz)	8.2	10.0	14.6	22.7	30.2	2.38	1.96	6.41	3.81	4.13	3.738
DS_2 (Moderate damage, Hz)	7.4	10.0	14.2	22	30	11.90	1.96	8.97	6.78	4.76	6.874
DS_3 (Heavily damage, Hz)	7.2	9.5	13.4	20.8	27	14.29	6.86	14.10	11.86	14.29	12.28

Table 4 Transversal frequency of URB

Damage State	f_1	f_2	f_3	f_4	f_5	Δf_1 (%)	Δf_2 (%)	Δf_3 (%)	Δf_4 (%)	Δf_5 (%)	Avg. Δf
DS_0 (Undamaged, before test, Hz)	9.0	12.4	16.3	19.0	27.0	-	-	-	-	-	-
DS_1 (Slight damage, Hz)	8.2	12.0	16.1	18.5	26.1	8.89	3.23	1.23	2.63	3.33	3.862
DS_2 (Moderate damage, Hz)	8.0	11.6	15.6	17.7	25.7	11.11	6.45	4.29	6.84	4.81	4.700
DS_3 (Heavily damage, Hz)	3.1	8.5	12.5	16.6	24.0	65.56	31.45	23.31	12.63	11.11	28.812

(a) (b) (c) (d)

Fig. 16 Out-of-plane damage evolution of URB model (a) 75 years return period, (b) 225 years return period, (c) 475 years return period, (d) 975 years return period

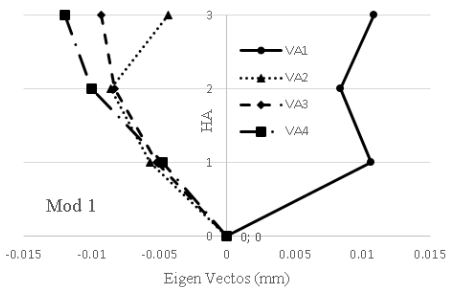

(a) Mode-1

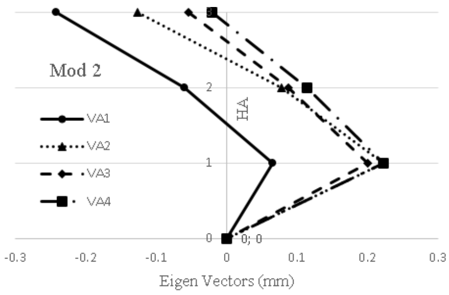

(b) Mode-2

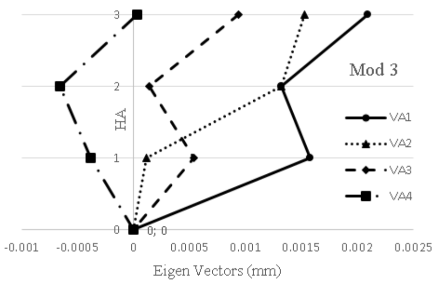

(c) Mode-3

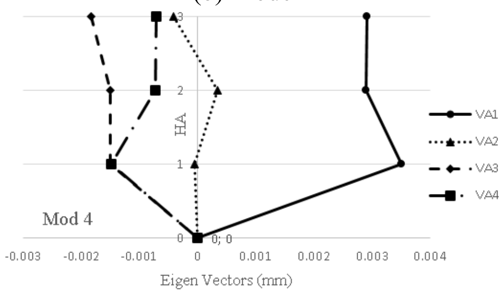

(d) Mode-4

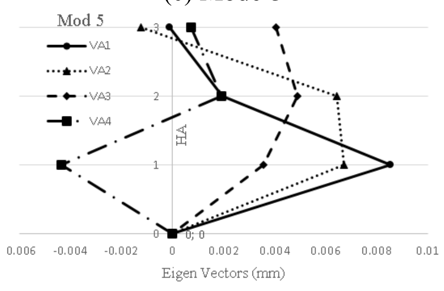

(e) Mode-5

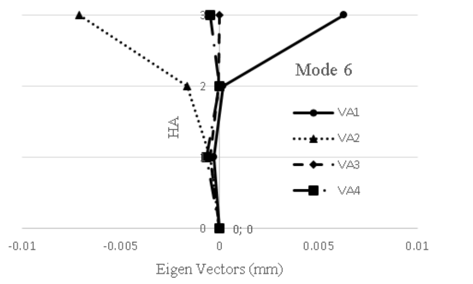

(f) Mode-6

Fig. 17 Mode shape evolution after seismic test for URB model

Table 5 Longitudinal frequency of BJR

Damage State	f_1	f_2	f_3	f_4	f_5	Δf_1 (%)	Δf_2 (%)	Δf_3 (%)	Δf_4 (%)	Δf_5 (%)	Avg. Δf (%)
DS_0 (Undamaged, before test, Hz)	7.3	9.9	14.6	17	27.3	-	-	-	-	-	-
DS_1 (Slight damage, Hz)	7.2	9.9	13.6	16.6	27.1	1.37	0.00	6.85	2.35	0.73	2.26
DS_2 (Moderate damage, Hz)	6.4	9.6	12.5	15.7	26	12.33	3.03	14.38	7.65	4.76	8.43
DS_3 (Heavily damage, Hz)	6.3	9.4	12.3	15	25	13.70	5.05	15.75	11.76	8.42	10.94

Table 6 Longitudinal frequency of BJR

Damage State	f_1	f_2	f_3	f_4	f_5	Δf_1 (%)	Δf_2 (%)	Δf_3 (%)	Δf_4 (%)	Δf_5 (%)	Avg. Δf (%)
DS_0 (Undamaged, before test, Hz)	8.15	9.23	13.60	19.00	26.00	-	-	-	-	-	-
DS_1 (Slight damage, Hz)	7.54	9.20	13.30	18.70	25.00	7.48	0.33	2.21	1.58	3.85	3.09
DS_2 (Moderate damage, Hz)	6.23	8.20	12.30	17.50	24.10	23.56	11.16	9.56	7.89	7.31	11.90
DS_3 (Heavily damage, Hz)	2.97	5.51	8.15	14.60	19.60	63.56	40.30	40.07	23.16	24.62	38.34

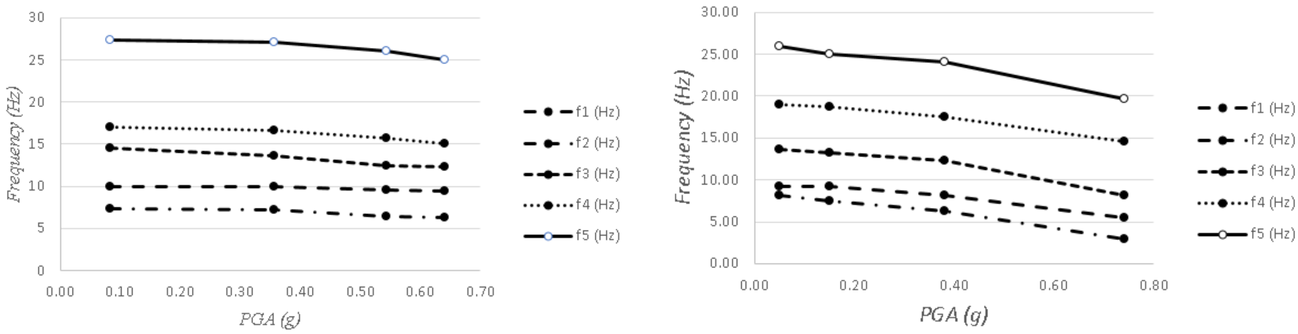

(a) In-Plane BJR (b) Out-of-plane BJR

Fig. 18 Frequency change of BJR for five modes during in-plane and out-of-plane excitation

2475 years return period and this drop percent is 65.56%. Average frequency decrease after second seismic test is 3.738%, after third seismic test is 6.874% and after fourth test is 12.28% through in-plane direction as presented in Table 3. In addition, on average, 3.862% frequency decrease was calculated after seismic excitation with 225 years return period. Then, 28.812% average frequency decrease was calculated after strong shaking with 2475 return period as tabulated in Table 4. The damage of the tested URB specimen after the seismic sequence test is presented in Fig. 16.

Damages of the infill wall started to propagate with lateral cracks, then these cracks were combined with spalling of plaster on the bricks. Main vibrations were measured on the boundary of infill with RCF. Brick fragments were spalled through out-of-plane direction of the infill wall at last stage of the experiment. This out-of-plane spalling loosened the infill wall; therefore, mode shapes were changed. Mode shape evolution can be seen in Fig. 17 due to the presented damage on the infill wall.

Fig. 17 presents that mode shapes radically changed at Mode-1 due to the spalling of plaster and damage of brick as seen in Fig. 15 (c) and (d). Decreased resistivity through out-of-plane direction caused discrepancy of movement of infill wall as seen in Fig. 17 (d) and (e). Damage of the infill wall can especially be seen HA1 at Mode 2. First crack occurred between the HA1 and HA2 at Model-1. These cracks then propagated and started spalling. This spalling caused detachment of infill wall and RCF. This detachment was observed at VA1, VA3 and VA4 at Eigenvector evolution at Mode 3. Once maximum out-of-plane displacement was reached on HA1, damage accumulation was observed on infill wall especially on the VA1, VA2 and VA3. VA4 is located on the free side of specimen as seen in Fig. 16 (c) and (d). Free side means, far location from Strut. Due to damage of bed joint and head joint of the brick, eigen vector evolution was observed through reverse direction of infill wall.

4.1 Model-II: BJR

The purpose of using bed joint reinforcement between two brick layers is to contribute ductility to the infill wall through out-of-plane direction to prevent total collapse and to increase in-plane bearing capacity. This ductility will prevent out-of-plane failure after a strong shaking. This result can be observed from frequency decrease of the tested specimen. Out-of-plane damage of the infill wall is mostly affected by in-plane damage. Bed joint reinforcement was placed between each two brick layers on infill wall. Bed joint reinforcement causes also friction and this friction increases in-plane bearing capacity and can be seen at mode frequencies evolution especially at first three modes. Mode frequencies and frequency decrease were presented in Fig. 18 (a) and (b).

Tables 5 and 6 present five frequencies and frequency decrease of BJR specimen after each phase of shaking table experiment. Average frequency decreases of the five modes of BJR model after 225 years return period are 2.26% and 3.09% through in-plane and out-of-plane direction,


(a) Damage of BJR model after 225 years return period earthquake load


(b) Damage of BJR model after 475 years return period earthquake load

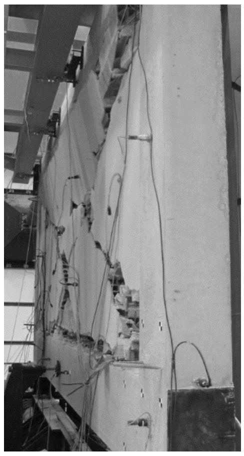
(c) Damage of BJR model after 2475 years return period earthquake load

Fig. 19 Damage evolution of BJR model under combined earthquake loading

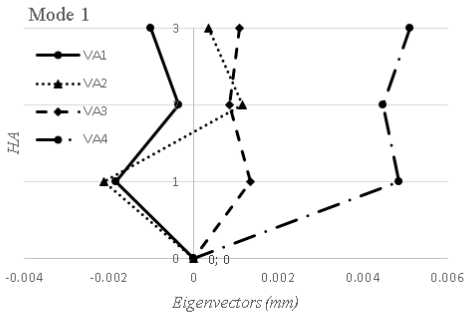

(a) Mode-1

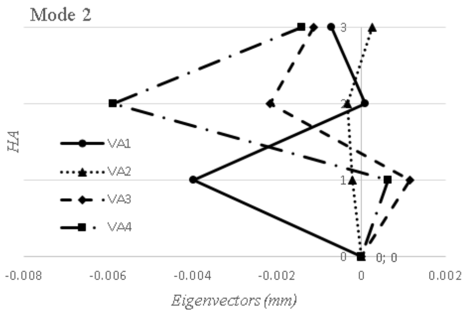

(b) Mode-2

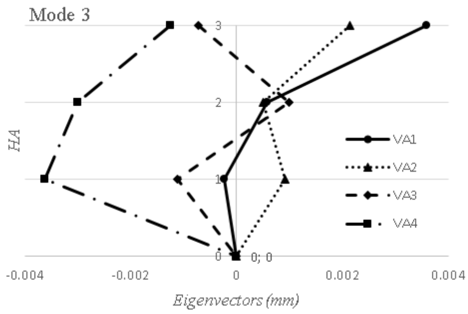

(c) Mode-3

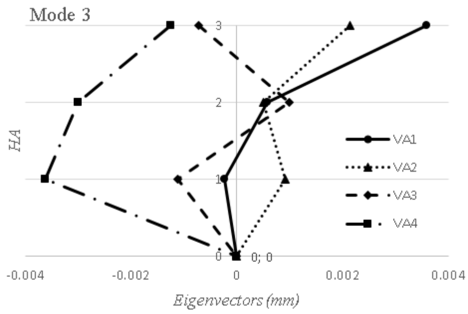

(d) Mode-4

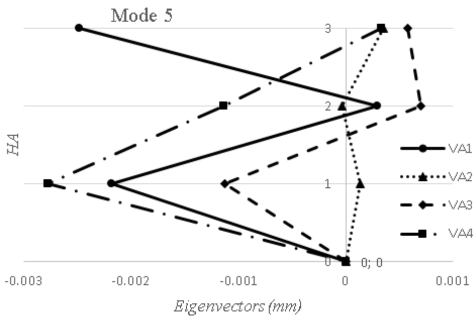

(e) Mode-5

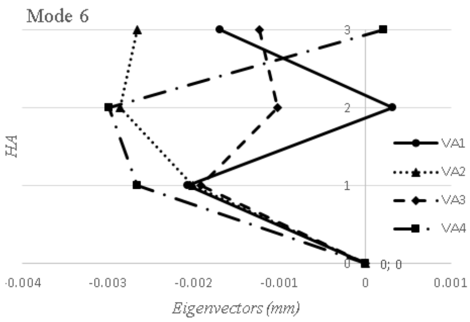

(f) Mode-6

Fig. 20 Mode shape evolution after seismic test for BJR model

respectively. Then, frequency decrease increased to 8.43% and 11.90% through in-plane and out-of-plane direction, respectively. In-plane frequency decrease is lower than out-of-plane frequency decrease up to 2%. However, frequency discrepancy between the in-plane and out-of-plane direction increased nearly to 27% after 2475 years return period earthquake excitation. Damage evolution of BJR model can be seen in Fig. 19.

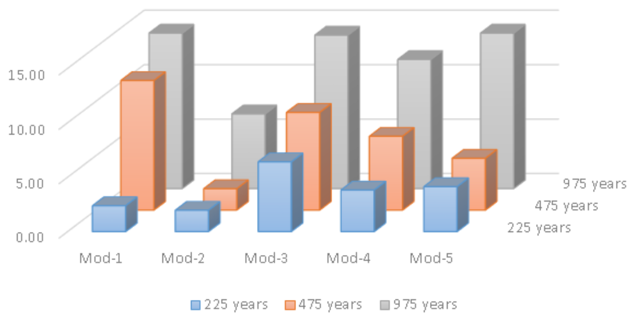

(a)

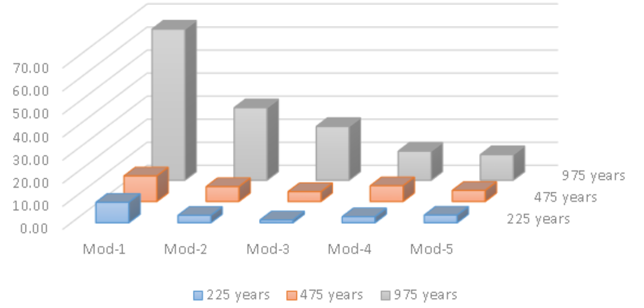

(b)

Fig. 21 Increase of damage for URB model, (a) IP direction, (b) OOP direction

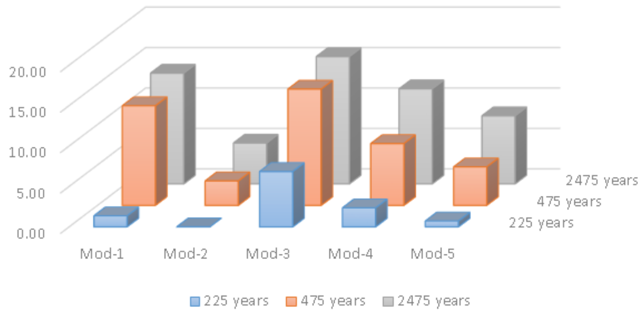

(a)

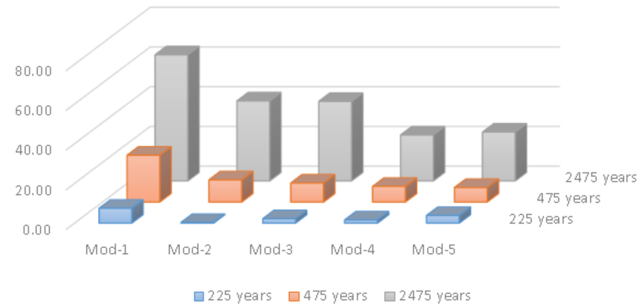

(b)

Fig. 22 Increase of damage for BJR model, (a) IP direction, (b) OOP direction

Local damage of the infill wall changed the mode shape of the infill wall as presented below.

Damage and cracks of the infill wall accumulated through a horizontal line at mid-part of the URB model, whereas the damages of the infill wall started to propagate the boundary of the infill wall and the RCF at bottom side of the BJR model as presented in Fig. 19 (a). In addition, bed joint reinforcement shows the ductile behavior under strong shaking. This behavior was proven by dynamic identification test as seen in Fig. 20 (b), (e) and (f).

5. Discussion

5.1 Model-I: URB

In this model (Model-I:URB), four dynamic identification tests were performed on the model with one undamaged and three damaged stages. Longitudinal, transversal and torsional modes were obtained. However, transversal modes were focused on to determine the effect of the in-plane damage on the out-of-plane damage which resulted together in a frequency decrease of the tested model. Fig. 21 (a) and (b) present the damage ratio on the base of mode direction. Vertical axis shows the damage in percent.

The frequency decrease of the URB model at the first five modes were 14.3% (f_1), 6.9% (f_2), 14.1% (f_3), 11.9% (f_4) and 14.3% (f_5) respectively compared to DS_3 (Heavily damaged) to DS_0 (Undamaged) state through in-plane direction. Moreover, frequency decrease is widely measured, especially through out-of-plane direction, and these ratios were measured as 65.6% (f_1), 31.5% (f_2), 23.3% (f_3), 12.6% (f_4) and 11.1% (f_5) respectively for URB model. The highest frequency decrease was observed at the first vibration mode through out-of-plane direction. Kocak and Yıldırım (2011) reported that there is a 33%-37% frequency difference between the bare frame and frame with infill wall for RCF structures, frequency decrease reached maximum 14.3% through in-plane direction and 65.6% through out-of-plane direction. Even if in-plane resistivity is still sustained, out-of-plane resistivity was exceeded end of the seismic test with a 2475 years return period.

5.2 Model-II: BJR

The second model consist of bed joint reinforcement to prevent total collapse of the structure. Bed joint reinforcement has not affected mode shapes, which was also due to tight connection with RC columns. Likewise, three mode shapes were observed such as longitudinal, transversal and torsional. Transversal mode shapes were focused on to compare contribution of bed joint reinforcement on BJR model compared with URB model. Fig. 22 presents the damage increase in percent-frequency relationship on the base of dynamic identification end of the seismic sequence.

Frequency decreases at BJR model through in-plane direction were measured as 13.7% (f_1), 5.1% (f_2), 15.7% (f_3), 11.8% (f_4) and 8.4% (f_5) for the first five modes, respectively. After the four seismic sequence, frequency decrease was measured for BJR model through out-of-plane direction were 63.6% (f_1), 40.3% (f_2), 40.1% (f_3), 23.2% (f_4) and 24.6% (f_5). These results present that bed joint reinforcement provided bond slip during the excitation and increased the in-plane bearing capacity as reported by Onat

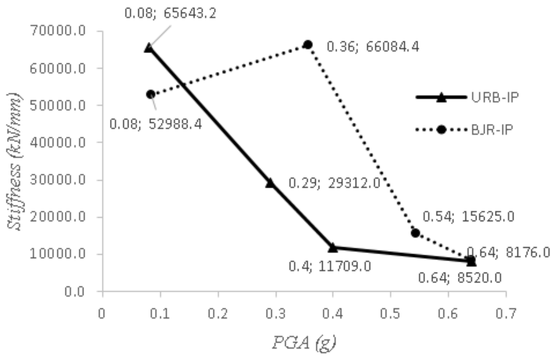

(a) In-plane stiffness-PGA

(b) Out-of-plane stiffness-PGA

Fig. 23 In-plane and out-of-plane stiffness-PGA change during the shaking table

et al. (2015, 2016). However, damage of the infill wall was not reflected by numeric results as expected. In-plane damage reached maximum 13.7% for first vibration mode. Moreover, out-of-plane damage caused maximum 63.6% frequency decrease for BJR model. Even if calculated frequency decrease is under expected result, BJR prevented total collapse of infill wall as presented in Fig. 19.

5.3 Overall analysis

Stiffness of the tested models needs to be evaluated to assess frequency decrease of the both models. For this purpose, Fig. 23 was plotted.

A lower stiffness degradation occurred abruptly at the URB model and was followed by a slight decrease. As for the BJR model, there was an increase after first test. The reason of this increase in stiffness is the presence of the BJR between the brick layers then the drop was steeper between the second and the third tests (Second test represents the dynamic identification tests after seismic tests with return periods of 225 years and third test represents the dynamic identification tests after seismic tests with return periods of 475 years, respectively) meaning that within this interval, the structure suffered a higher damage as presented in Fig. 16 and Fig. 19. The damage observed in the model steadily increased over the seismic sequence, the first damage being visually observed for a return period of 225 years, with the detachment of brick and RCF. Before the test of return period of 225 years, only lateral cracks were observed on the plaster for both

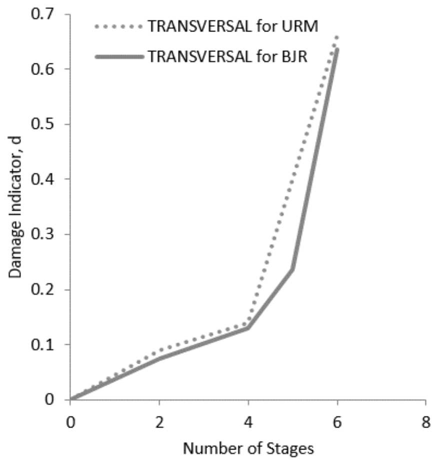

Fig. 24 Damage index for both models through out-of-plane direction

models through in-plane direction.

The lowest stiffness drop occurred in BJR model after the test return period of 475 years followed by URB model through in-plane direction. An increase was observed for both model after the first quake, then in URB and BJR model the drop was steeper between the second and the third dynamic identifications which correspond to the seismic identification tests after the seismic tests with return periods of 225 and 475 years, respectively. This means that within this interval the structure suffered a higher damage. After all data is investigated, it can be concluded that the structural vulnerability of tested specimen can be better understood from the first vibration mode. An increase was observed in stiffness after second test for BJR specimen and the same increase was observed after first test for URB specimens. The reason of this increase is applied earthquake load in narrow band high frequency. The infill walls resisted with its total capacity through out-of-plane direction. To show the structural vulnerability in a better way, damage index parameter was evaluated for both of the specimens.

To evaluate the structural vulnerability of the infill walls in terms of in-plane and out of-plane. There is a basic relation between damage indicator, mass, stiffness and frequency of a SDOF system. To demonstrate progressive damage of infill wall, damage index was used.

$$d_n = 1 - \frac{f_i}{f_1} \tag{1}$$

Where subscript, n indicates the stage, f indicates the frequency of mode i in the dynamic identification test n. It is further assumed that the damage is isotropic between the 1^{st} and the n^{th} dynamic identification tests.

This damage index will vary linearly with the frequency of the nth dynamic identification test between 0, meaning no damage, and 1, representing total collapse. The evolution of this damage index for the 1st vibration mode of both specimens is shown in Fig. 24. As observed, both models experience a similar evolution of this damage index for out-of-plane direction.

However, BJR model provided ductility to specimen and prevented total collapse as seen in Fig. 24. Obtained results in this study showed similar frequency decrease with

Goncalves *et al.*'s (2018) study. In their study, 50% frequency decrease was obtained from unreinforced Pombalio (This type of building composed of a timber frame with vertical and horizontal elements, braced with diagonals and masonry infill.) type building and 70% frequency decrease with reinforced Pombalio building. In their study dominant frequency interval after damage are 2.5 Hz and 5 Hz. Moreover, in this study dominant frequency interval are 2.97 Hz for URB model and 3.1 Hz for BJR model through out-of-plane direction.

6. Conclusions

This paper aimed at investigating frequency decrease-damage relationship on the base of shaking table experiment results. Then, frequency decrease and stiffness degradation were evaluated with applied Peak Ground Acceleration (PGA) by considering the strength deterioration. Finally, eigenvector change-local damage and eigenvector change-frequency relationship were investigated. On the base of investigation, concluding remarks were listed below;

- Mode shapes evolution in transversal direction occurred due to the detachment of infill wall from RCF especially at URB model. For this reason, local leaps were observed at the top of the eigenvectors.
- Bed joint reinforcement contributes ductility to infill wall. However, mode shapes evolution showed a jump especially between the HA2 and HA3. This means that the infill wall with bed joint reinforcement shows ductile behavior
- The steepest frequency decrease was observed at the first mode. For this reason, damage and frequency decrease relationship were focused on at the first mode.
- Infill wall continued to resist to the frame at end of the shaking table experiment through in-plane direction. However, the infill wall lost the bearing capacity through out-of-plane direction at end of the test for both of the model.
- The damage in the models were assessed on the base of relative loss of mode frequency ratios considering that the damage was completely related to the stiffness variation of the tested models.
- On the base of the frequency decrease, it can be reported that bed joint reinforcement contributes stiffness to infill wall at the early stage of the tests. After medium damage state, stiffness of the BJR model decreased steeper.
- Due to material deterioration during seismic action and increased stiffness of the model, bed joint reinforcement application can provide successful results until 2475 years return period earthquake load.
- Finally, damage index proved that bed joint reinforcement protects infill from total collapse.

References

Al-Nimry, H., Resheidat, M. and Al-Jamal, M. (2014), "Ambient vibration testing of low and medium rise infilled RC frame buildings in Jordan", *Soil Dyn. Earthq. Eng.*, **59**, 21-29.

Altunışık, A.C., Bayraktar, A. and Sevim, B. (2011), "Output-only system identification of post tensioned segmental concrete highway bridge", *J. Bridge Eng.*, **16**(2), 259-266.

Amanat, K.M. and Hoque, E. (2006), "A rationale for determining the natural period of RC building frames having infill", *Eng. Struct.*, **28**(4), 495-502.

Asteris, P.G., Repapis, C.C., Cavaleri, L., Sarhosis, V. and Athanasopoulou, A. (2015), "On the fundamental period of infilled RC frame buildings", *Struct. Eng. Mech.*, **54**(6), 1175-1200.

Asteris, P.G., Repapis, C.C., Tsaris, A.K., Di Trapani, F. and Cavaleri, L. (2015), "Parameters affecting the fundamental period of infilled RC frame structures", *Earthq. Struct.*, **9**(5), 999-1028.

Chiauzzi, L., Masi, A., Mucciarelli, M., Cassidy, J.F., Kutyn, K., Traber, J., Ventura C. and Yao, F. (2012), "Estimate of fundamental period of reinforced concrete buildings: code provisions vs. experimental measures in Victoria and Vancouver (BC, Canada)", *Proceedings of the 15th World Conference on Earthquake Engineering*, Vol. 3033, Lisboa.

Chopra, A.K. and Goel, R.K. (2000), "Building period formulas for estimating seismic displacements", *Earthq. Spectra* **16**(2), 533-536.

Crowley, H. and Pinho, R. (2004), "Period-height relationship for existing european reinforced concrete buildings", *J. Earthq. Eng.*, **8**(1), 93-119.

Ditommaso, R., Gallipoli, M.R. and Mucciarelli, M. (2013), "Evaluation and considerations about fundamental periods of damaged reinforced concrete buildings", *Nat. Hazard. Earth Syst. Sci.*, **13**(7), 1903.

Eleftheriadou, A.K., Karabinis, A.I. and Baltzopoulou, A.D. (2012), "Fundamental period versus seismic damage for reinforced concrete buildings", *Proceedings of the 15th World Conference on Earthquake Engineering*, Lisboa.

Foti, D., Gattulli, V. and Potenza, F. (2014), "Output-only identification and model updating by dynamic testing in unfavorable conditions of a seismically damaged building", *Comput. Aid. Civil Infrastr. Eng.*, **29**(9), 659-675.

Gallipoli, M.R., Mucciarelli, M. and Vona, M. (2009), "Empirical estimate of fundamental frequencies and damping for Italian buildings", *Earthq. Eng. Struct. Dyn.*, **38**(8), 973-988.

Goel, R.K. and Chopra, A.K. (1997), "Period formulas for moment-resisting frame buildings", *J. Struct. Eng.*, ASCE, **123**(11), 1454-1461.

Goel, R.K. and Chopra, A.K. (1998), "Period formulas for concrete shear wall buildings", *J. Struct. Eng.*, ASCE, **124**(4), 426-433.

Goncalves, A.M.N., Guerreiro, L.M.C., Candeias, P., Ferreira, J.G. and Costa, A.C. (2018), "Characterization of reinforced timber masonry walls in "Pombalino" buildings with dynamic tests", *Eng. Struct.*, **166**, 93-106.

Guler, K., Yuksel, E. and Kocak, A. (2008), "Estimation of the fundamental vibration period of existing RC buildings in Turkey utilizing ambient vibration records", *J. Earthq. Eng.*, **12**(S2), 140-150.

Koçak, A. and Yıldırım, M.K. (2011), "Effects of infill wall ratio on the period of reinforced concrete framed buildings", *Adv. Struct. Eng.*, **14**(5), 731-743.

Kocak, A., Borekci, M. and Zengin, B. (2018), "Period formula for RC frame buildings considering infill wall thickness and elasticity modulus", *Scientia Iranica. Tran. A, Civil Eng.*, **25**(1), 118-128.

Leite, J.K. (2014), "Seismic behaviour of infill walls: Design and testing", PhD Thesis, Universidade of Minho, Guimaraés, Portugal,.

Leite, J.M., Correia, A.A., Lourenço, P.B., Vintzileou, E., Palieraki, V., Candeias, P.X., Campos-Costa, A. and Coelho, E.

(2015), “Assessment of innovative solutions for non-load bearing masonry enclosures”, Chapter 16 of Experimental Research in Earthquake Engineering, Ed. F. Taucer, Springer Bbook Series Geotechnical, Geological and Earthquake Engineering.

Masi, A. and Vona, M. (2010), “Experimental and numerical evaluation of the fundamental period of undamaged and damaged RC framed buildings”, *Bull. Earthq. Eng.*, **8**(3), 643-656.

Mendes, P. and Oliveira, S. (2008), “Análise dinâmica de estruturas. Utilização integrada de modelos de identificação modal e modelos de elementos finitos”, ITB ADE 16, Laboratório Nacional de Engenharia Civil, Lisboa. (in Portuguese)

Onat, O. (2019), “Fundamental vibration frequency prediction of historical masonry bridges”, *Struct. Eng. Mech.*, **69**(2), 155-162.

Onat, O. and Gul, M. (2018), “Application of Artificial Neural Networks to the prediction of out-of-plane response of infill walls subjected to shake table”, *Smart Struct. Syst.*, **21**(4), 521-535.

Onat, O., Correia, A.A., Lourenço, P.B. and Koçak, A. (2018), “Assessment of the combined in-plane and out-of-plane behavior of brick infill walls within reinforced concrete frames under seismic loading”, *Earthq. Eng. Struct. Dyn.*, **47**(14), 2821-2839.

Onat, O., Lourenco, P.B. and Kocak, A. (2015), “Experimental and numerical analysis of RC structure with two leaf cavity wall subjected to shake table”, *Struct. Eng. Mech.*, **55**(5), 1037-1053.

Onat, O., Lourenco, P.B. and Kocak, A. (2016), “Nonlinear analysis of RC structure with massive infill wall exposed to shake table”, *Earthq. Struct.*, **10**(4), 811-828.

Onat, O., Lourenço, P.B. and Koçak, A. (2017), “Structural model calibration of RC structure with two-leaf cavity brick infill wall by deterministic approach”, *Građevinar*, **69**(3), 171-181.

Salameh, C., Guillier, B., Harb, J., Cornou, C., Bard, P.Y., Voisin, C. and Mariscal, A. (2016), “Seismic response of Beirut (Lebanon) buildings: instrumental results from ambient vibrations”, *Bull. Earthq. Eng.*, **14**(10), 2705-2730.

Sevim, B., Bayraktar, A. and Altunişik, A.C. (2011a), “Finite element model calibration of berke arch dam using operational modal testing”, *J. Vib. Control*, **17**(7), 1065-1079.

Sevim, B., Bayraktar, A., Altunişik, A.C., Atamtürktür, S. and Birinci, F. (2011b), “Assessment of nonlinear seismic performance of a restored historical arch bridge using ambient vibrations”, *Nonlin. Dyn.*, **63**(4), 755-770.

Su, R.K.L., Lee, C.L. and Wang, Y.P. (2012), “Seismic spectral acceleration assessment of masonry in-filled reinforced concrete buildings by a coefficient-based method”, *Struct. Eng. Mech.*, **41**(4), 479-494.

URL1:http://www.lnec.pt/estruturas/pt/nucleo/nucleo-de-engenharia-sismica-e-dinamica-de-estruturas/apresentacao-1/

Vidal, F., Navarro, M., Aranda, C. and Enomoto, T. (2014), “Changes in dynamic characteristics of Lorca RC buildings from pre-and post-earthquake ambient vibration data”, *Bull. Earthq. Eng.*, **12**(5), 2095-2110.

Yu, J., Zhang, Y. and Lu, Z. (2014), “Seismic rehabilitation of RC frame using epoxy injection technique tested on shaking table”, *Struct. Eng. Mech.*, **52**(3), 541-558.

Zhang, X.C., Xue, J.Y., Zhao, H.T. and Sui, Y. (2011), “Experimental study on Chinese ancient timber-frame building by shaking table test”, *Struct. Eng. Mech.*, **40**(4), 453-469.

CC